

Modelling of Negative Skin Friction on Driven Piles

Osama Drbe, Abouzar Sadrekarimi & M. Hesham El Naggar
Department of Civil & Environmental Engineering – Western University
London, Ontario, Canada, N6A 5B9
Tony Sangiuliano
Ministry of Transportation Ontario, Toronto, ON, Canada



ABSTRACT

Dragload and dragdown are engineering problems that are encountered in designing piles in soft cohesive soils. A pile installed in soft soil can be subjected to additional frictional loads resulting from the relative movement between the adjacent soft soil and the pile. This movement creates negative skin friction along the upper part of the pile above the neutral plane, which is resisted by positive skin friction along the lower segment of the pile below the neutral plane. In this paper, finite element analyses are carried out to model negative skin friction mobilized on driven piles installed in soft clay. The location of the neutral plane and the effects of pile length and coating on the neutral plane location are investigated. The numerical model is compared with field data from instrumented coated and uncoated hollow-cylindrical pre-stressed concrete piles driven into soft Bangkok clay. The negative skin friction predicted from the numerical analyses agrees reasonably well with field measurements. The analyses results suggest that the location of neutral plane changes with pile length, coating, and vertical loading. Using β that varies with depth yields to better estimation of dragloads comparing with using a constant value of β .

RÉSUMÉ

Faites glisser et faites-le glisser vers le bas de charge sont des problèmes d'ingénierie qui sont rencontrés en concevant des tas dans les sols tendres et cohésifs. Un tas qui est installé dans le sol tendre peut être assujéti aux charges de frottement supplémentaires qui sont le résultat du mouvement relatif entre le tas et le sol tendre adjacent. Ce mouvement crée la résistance de frottement négative le long de la partie supérieure du tas, qui est résisté à la résistance de frottement positive le long de la partie inférieure du tas avec la résistance au basculement. Dans ce document, l'analyse par éléments finis (AEF) est effectuée pour modéliser la résistance de frottement négative qui est mobilisée sur des tas entraînés installés dans l'argile tendre. La résistance de frottement négative qui était prévu de l'analyse numérique est d'accord raisonnablement avec les mesures du champ. Les résultats de l'analyse suggèrent que l'emplacement du plain neutre change quand la longueur, l'enduit et le chargement vertical du tas changent. En utilisant β qui varie en fonction de la profondeur pour mieux estimer les rendements de traînée comparant les charges à l'aide d'une valeur constante de β .

1 INTRODUCTION

Urban development has led to building higher and larger structures including skyscrapers and bridges. Loads of these massive structures are transferred to deeper and stronger soil layers where adequate support is available. Deep foundation units comprised of driven or bored piles are used to support structures such as buildings and bridges. Deep foundation units derive their supporting capacity from shaft by means of skin friction and/or tip resistance.

At sites where a pile is driven through compressible soils such as soft clay, and settlement of the soil adjacent to the pile is caused by external loadings such as an approach embankment to a bridge and/or an abutment, the relative movement of the soil adjacent to the pile will cause negative skin friction. This frictional force mobilized with a few millimeters of relative displacement at the pile-soil interface. The location of force equilibrium is often called the "neutral plane", which can be defined as the plane where soil settlement and pile displacement become equal, skin friction becomes zero, or the maximum axial load is developed. "Downdrag" is defined as the downward settlement of a pile from the dragging force exerted by the adjacent soft soil, while "dragload" is the load transferred

on a pile from negative skin friction (Fellenius 2015). Negative skin friction may cause structural distress to the pile as it induces an additional load (dragload) on a pile installed in a compressible soil. This additional load can reduce the pile structural capacity and compromises its serviceability (Poulos 1979).

Numerous studies have investigated the effect of negative skin friction on piles through full-scale field tests, centrifuge model tests on small piles, and analytical/numerical analysis. In this paper, a numerical finite element analysis is carried out using Plaxis 2D (Ver. AE.02) to model instrumented pile tests described by Indraratna et al. (1992). The numerical model is then used to study the location of the neutral plane and the effects of pile coating, length, and pile load on the location of neutral plane.

2 CASE STUDY

Indraratna et al. (1992) describe the field behaviour of coated and uncoated instrumented hollow cylindrical pre-stressed concrete piles driven into soft clay in a site located 10 km east of Bangkok City. The subsurface conation, installation and configuration of the piles, instrumentations,

and monitoring program will be discussed in the following subsections.

2.1 Subsurface Condition

The subsurface condition of Bangkok plain is mainly composed of low strength and highly compressible soft soil (Balasubramaniam et al. 2009), which overlies a medium to stiff clay and dense sand layers. Boreholes at the site indicated 2 - 4 m of overconsolidated weathered clay overlying a soft clay layer that extends to a depth of 20 m. A medium-stiff to stiff clay layer with a thickness of 6 - 8 m was encountered at the bottom of the boreholes. The water table was located at a depth of 2 m from the ground surface. Figure 1 shows the corresponding subsoil profile adopted in the numerical analysis.

Strength tests showed that the undrained shear strength varies between 20 - 45 kPa for the weathered clay layer, and 16 - 38 kPa for the soft clay layer. The average value of undrained shear strength for the medium stiff to stiff clay layer is 45 kPa.

Index tests showed that the water content of the weathered clay varies from 40% above the water table to 55% below the water table. The water content of the soft clay layer varies from depth to depth and it reaches 95% at some depths. The soft clay layer has a liquid limit range of 70% - 100% and plastic limit range of 25% - 40%. The compression index of the soft clay is between 1.1 - 1.3. The Modified Cam Clay (MCC) parameters for the subsurface soils are listed in Table 1.

2.2 Pile Configuration and Installation

Each pile has an outer diameter of 400 mm and an internal diameter of 250 mm and consisted of 5 segments. Both piles were driven to a depth of 25 m. First, two segments of each pile were connected to each other, and they were then driven by means of dropping a 6000 kg hammer with a driving rate of 1m/min. Next, the third segment was connected to the installed segments and driven using the 6000 kg hammer. The same process was repeated for the remaining segments. The top 4 segments of one of the piles was coated with 6 mm thickness of bitumen, while the other pile was left uncoated.

2.3 Field Instrumentation

Field monitoring included instrumentation of piles as well as the adjacent soil (Indraratna et al. 1992). The piles were instrumented with load cells, telltales, and LVDTs. Load cells were placed at the piles' tip and along the piles length. Load cells were used to measure the load transferred along the pile length. A telltale system was used to measure pile deformation (compression), and LVDTs were employed to measure the total settlement of the piles. In addition, piezometers were installed beside each load cell to measure changes in pore water pressure at the pile-soil interface.

The soil was monitored employing surface settlement plates, deep settlement points, and piezometers. Settlement plates were used to measure the total settlement at the ground surface while the deep settlement

points were implemented to measure soil settlement at different depths. A series of additional "dummy" piezometers were also installed between the piles in order to measure excess pore water pressure within the soil and hence calculate changes in pore pressure at the pile-soil interface. The approximate locations of these instruments are illustrated in Figure 1.

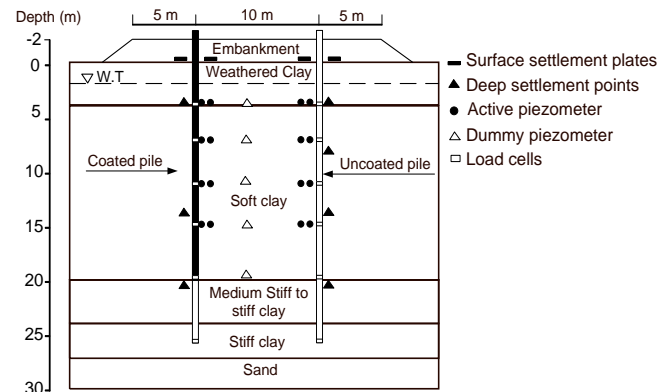


Figure 1. Soil profile and instrumentation layout (after Indraratna et al. 1992)

2.4 Monitoring program

Two phases of monitoring program were performed for each pile, short and long term monitoring programs. For the short term monitoring program, pullout tests were conducted after driving the piles to depths of 8, 12, 16, and 20 m. The purpose of these tests was to examine the suitability of using pullout testing for predicting negative skin friction. The second phase of monitoring started after constructing a 2 m high embankment and extended up to 9 months. The embankment was built in three days in order to apply a rapid load and induce settlement in the soil adjacent to the pile.

3 FINITE ELEMENT MODEL

In this paper, an axisymmetric numerical model is developed using Plaxis 2D in order to verify and predict the behaviour of the instrumented field piles. A model width of 5 m is adopted based on the results of a sensitivity analysis. 15-node triangle elements are used for modeling the soil and the pile. The 15-node triangle element provides an accurate fourth-order interpolation of displacement and numerical integration involving 12 stress points (Plaxis 2D 2012). A fine mesh is assigned around the pile and interface elements are used at the pile-soil interface. The model is assumed to be fixed at the bottom, and free to move vertically at the axisymmetric line and the outer boundary condition. No drainage is allowed at the axisymmetric line. Figure 2 shows the model used in the numerical analysis.

Table 1 MCC soil properties used in the model

Depth (m)	γ kN/m ³	e_o^*	$k \times 10^{-4}^*$ (m/day)	κ	λ	M	ν	OCR
0-4	16.7	1.8	1.3	0.053	0.182	1.05	0.2	3
4-10	14.7	2.8	5.5	0.084	0.514	0.97	0.2	1.3
10-20	16.7	2.4	2.6	0.063	0.323	0.98	0.2	1.3
20-30	18.6	1.2	1.1	0.027	0.116	0.9	0.2	1.85

* Values used by Indraratna and Chu, 2005

Table 2. Model parameters for the embankment (fill) and pile

Material	E (kPa)	ϕ' (degs)	γ (kN/m ³)	ν
Fill	4.9×10^3	30	16.7	0.2
Pile	2.9×10^7	---	24.5	0.2

Plaxis offers a variety of constitutive models and material properties. Based on the available data, the pile is modeled as a linear elastic material, while the soil layers are modeled using the Modified Cam Clay (MCC) model. However, the Mohr-Coulomb model is used to define the embankment fill properties. The model parameters for each soil layer are shown in Table 1 and the material parameters assigned to the fill and pile are shown in Table 2 where;

- γ = unit weight
- e_o = initial void ratio
- k = permeability
- κ = Cam-Clay swelling index
- λ = Cam-Clay compression index
- M = tangent of the critical state line
- ν = Poisson's ratio
- OCR = over consolidation ratio
- E = modulus of elasticity
- ϕ' = effective friction angle

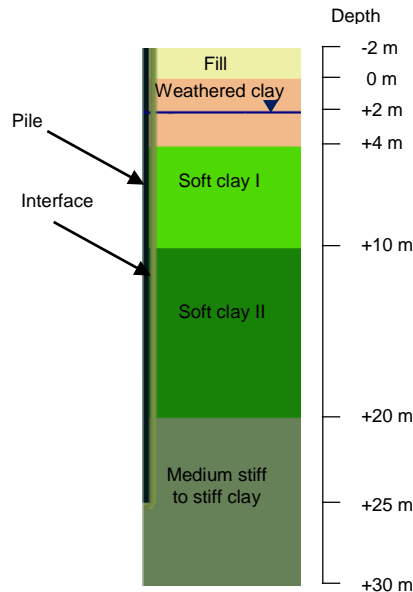


Figure 2. Finite element pile model in Plaxis 2D

It is worth mentioning that the adopted values of permeability (k) and void ratio (e_o) are determined from an airport site at the east of Bangkok City (Indraratna & Chu 2005) which is underlain by similar soil layers.

3.1 Interface Properties

As the consolidation settlement took place for long time (265 days), the drained parameters (effective stress parameters) control the pile-soil behaviour.

As a result of soil disturbance due to pile driving, the soil around the pile shaft would lose its cohesive strength. Therefore, frictional resistance would mobilize along the pile shaft, which is given by (Burland 1973):

$$\tau_s = K \sigma'_v \tan(\delta) \quad [1]$$

Where;

- τ_s = shaft frictional resistance
- σ'_v = vertical effective stress
- K = lateral earth pressure coefficient
- δ = friction angle mobilized at the soil-pile interface

The product of ($K \tan(\delta)$) is often taken as the β -parameter and thus Equation 1 is expressed as:

$$\tau_s = \beta \sigma'_v \quad [2]$$

For a normally-consolidated soft clay soil (Burland 1973)

$$\beta = (1 - \sin \phi'_r) \tan \phi'_r \quad [3]$$

Where ϕ'_r is the remolded friction angle at pile-soil interface.

For overconsolidated clays, Equation 3 is modified to account for the overconsolidation ratio (OCR), i.e.:

$$\beta = (1 - \sin \phi'_r) \tan \phi'_r \sqrt{OCR} \quad [4]$$

Burland (1973) found that $\beta = 0.20$ provided a good agreement between computed and measured negative skin friction for two driven steel piles. Whereas, $\beta = 0.25$ led to an upper limit of negative skin friction. The observations by Indraratna et al. (1992) agree with what was reported by Burland (1973) as shown in Figure 3. The value of β was found to be 0.25 and 0.20 as a maximum value and an average value for uncoated pile, respectively. Accordingly, $\beta = 0.20$ is adopted in the numerical analysis for the uncoated pile in this study.

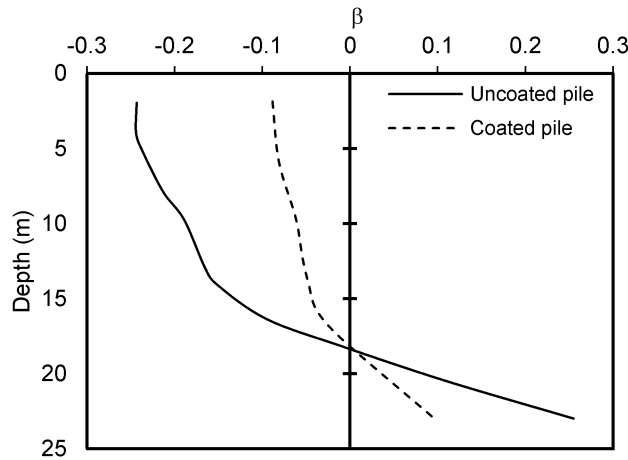


Figure 3. Observed variation of β with depth (after Indraratna et al. 1992)

3.2 Model Verification

The surface settlement of a point at a distance of 3.0 m from the uncoated pile is used to calibrate the model as it is believed that this point was not affected by pile installation. As shown in Figure 4, a good agreement is obtained between the numerical analysis and the measured surface settlement.

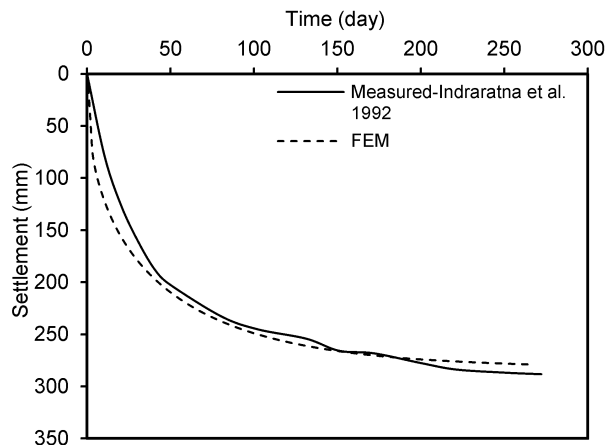


Figure 4. Measured and calculated surface settlement at a distance of 3 m away from the pile

In the following, numerical analysis results are compared with those observed from the instrumented piles after 262 days from the day of embankment construction. The ground settlement profile in Figure 5 shows a good agreement between the numerical analysis and those reported by Indraratna et al. (1992).

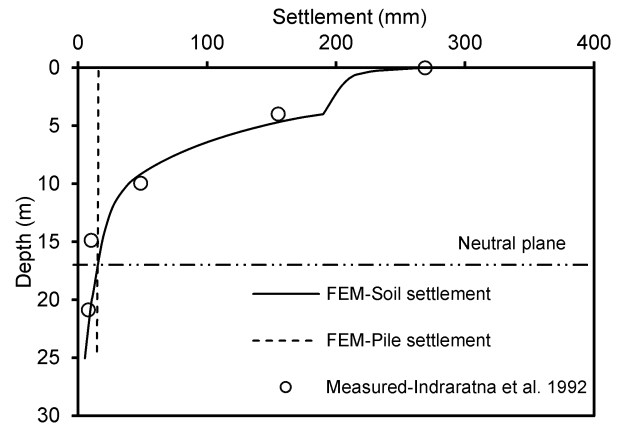


Figure 5. Settlement profiles at distance of 0.25 m from the pile centre

Figure 6 presents the distribution of skin friction along the uncoated pile shaft. As can be noted from Figure 6, the calculated skin friction agrees reasonably with skin friction measured along the pile shaft. Despite the good agreements observed in Figures 5 and 6, the numerical model tends to slightly overestimate the axial load developed along the pile shaft as demonstrated in Figure 7.

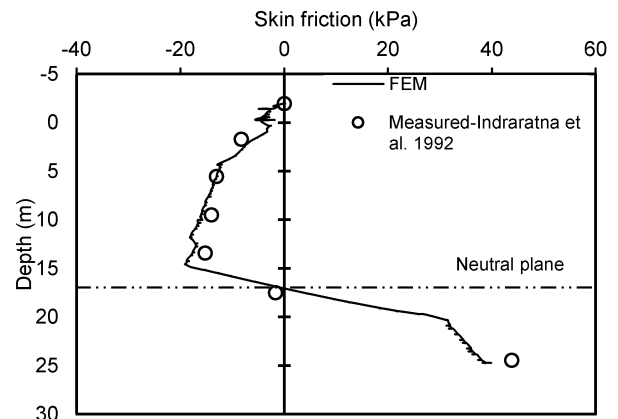


Figure 6. Skin friction distribution on the uncoated pile using constant β

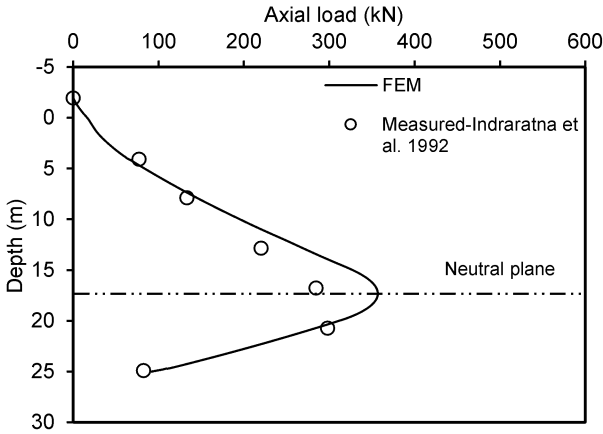


Figure 7. Axial load distribution along the uncoated pile length using constant β

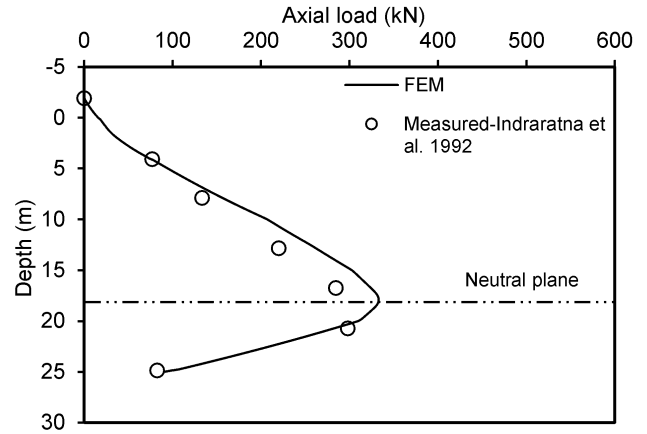


Figure 9. Axial load distribution along the uncoated pile length using β that varies with depth

Figures 8 and 9 present the distributions of skin friction and axial load along the uncoated pile using β that varies with depth. The Figures show that good agreements were found between the numerical results and the measured values of skin friction, axial load and the location of the neutral plane. Comparing the two sets of analyses (constant β and β varies with depth), it can be observed that the assumption of β that varies with depth gives more reasonable results as shown in Figures 8 and 9.

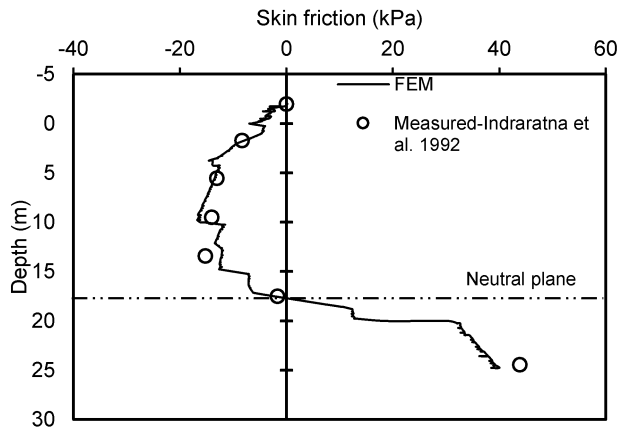


Figure 8. Skin friction distribution on the uncoated pile using β that varies with depth

The numerical analysis was further repeated for the coated pile. Pile coating is replicated by adopting $\beta = 0.05$ for soft clay, and 0.07 for medium stiff to stiff clay, which provided dragloads (in Fig. 10) very close to those measured on the instrumented coated pile. The β values were obtained from the field measurement reported by Indraratna et al. (1992). Comparison of Figures 9 and 10 suggests that pile coating was effective in reducing the dragload by about 60%.

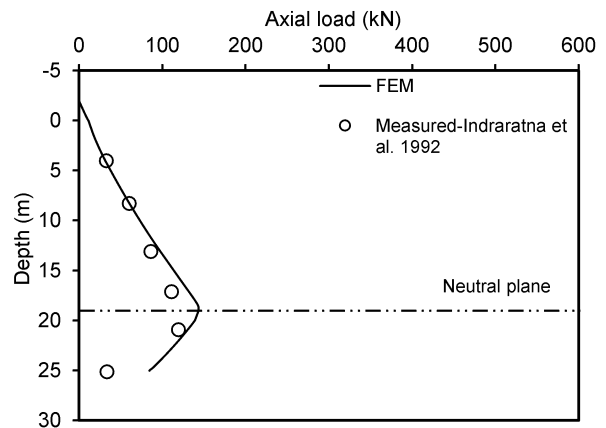


Figure 10. Axial load distribution along the coated pile length

Figures 6 to 10 shows negative value of depth because the ground surface level and the fill surface are assumed to be at depths of 0 m, and - 2 m, respectively.

4 DISCUSSION

A parametric study was performed using the developed model to examine the effect of pile length and coating on the location of the neutral plane using a constant of β for simplification.

4.1 Effect of Coating on the Neutral Plane

The numerical analyses results in Figures 6 and 7 show that the neutral plane is located at a depth of 17.2 m below the ground surface for the uncoated piles. This is close to those determined from the measurements of negative skin friction (18 m) or dragload (20 m) on the pile.

Pile coating would change the location of the neutral plane (Clemente 1981). According to Figures 10 and 11, coating not only reduced the negative skin friction, and

positive skin friction, but also shifted the neutral plane to a deeper depth of 18.8 below the ground surface (based on the FEM model). Similarly, Fellenius (2006) found that pile coating reduced the dragload and transferred the neutral plane to a deeper location.

It is believed that the coating shifted down the location of the neutral plane because the coated pile is subjected to less dragload and hence less pile settlement compared to the uncoated pile.

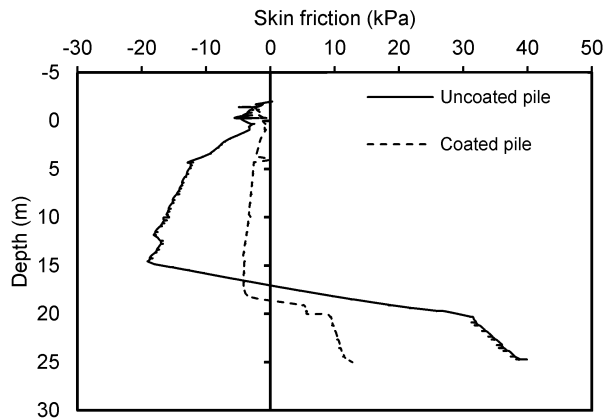


Figure 11. Effect of coating on the location of the neutral plane based on FEM analysis

4.2 Effect of Pile Length on the Neutral Plane

The effect of pile length is investigated by performing numerical analyses considering pile lengths of 15, 19, 23, and 27 m and the results are shown in Figure 12. It can be noted from Figure 12 that the location of the neutral plane tends to shift to a shallower depth with decreasing pile length. In addition, Figure 9 suggests that long piles carry more dragloads than short piles.

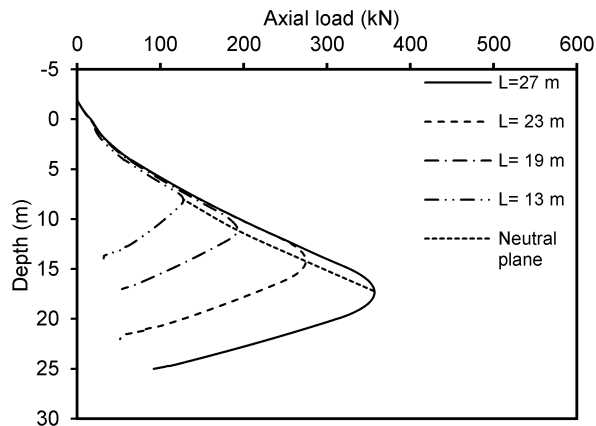


Figure 12. Effect of pile length on the location of the neutral plane for uncoated piles based on FEM analysis

4.3 Effect of Vertical loading on Neutral Plane Location

The change of neutral plane location is examined for an uncoated pile subjected to vertical loads of $P = 0, 150,$ and 300 kN as shown in Figure 13. For each case, the vertical load is applied in stages on the pile head at the end of embankment construction and the analysis is carried out for 262 days. The results show that the depth of neutral plane and thus the pile length subject to negative skin friction decreases with increasing the applied vertical load. This occurs because of two mechanisms: 1) the applied vertical load overcomes a part of the negative skin friction by mobilizing some positive skin friction, and 2) pile settlement resulting from the vertical load reduces the differential movement – responsible for developing negative skin friction – between the soil and the pile.

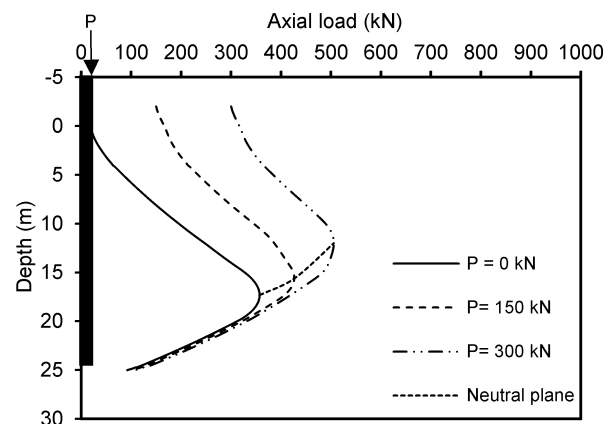


Figure 13 Effect of vertical loading on the location of the neutral plane for an uncoated pile based on FEM analysis

4.4 Effect of Dragload on Pile Settlement

Figures 14 and 15 compare the axial load distributions (“dragload”) and pile/soil settlements (“downdrag”) of uncoated and coated piles subject to a vertical load of 300 kN for 262 days after embankment construction. Despite the larger dragload (see Fig. 14) and the deeper neutral plane (see Fig. 15a) of the uncoated pile, it undergoes a significantly smaller settlement than the coated pile as shown in Figures 15a and 15b. In other words, although coating the entire length of a pile can be quite effective in reducing negative skin friction, it will also reduce the positive skin resistance, leading to a larger pile settlement. That’s why according to Fellenius (1997): “The larger the dragload, the stiffer, stronger and better the foundation, while in contrast, the larger the downdrag, the worse the foundation.”

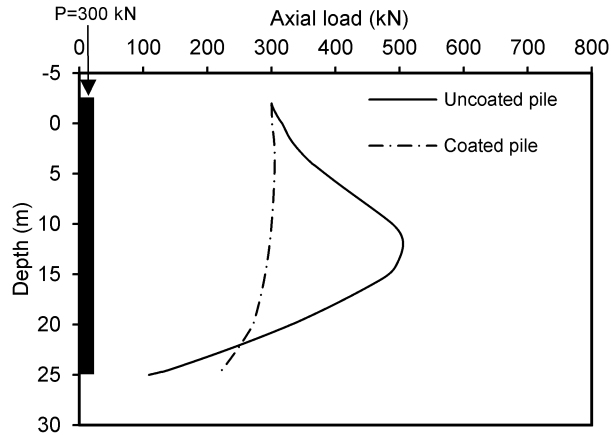
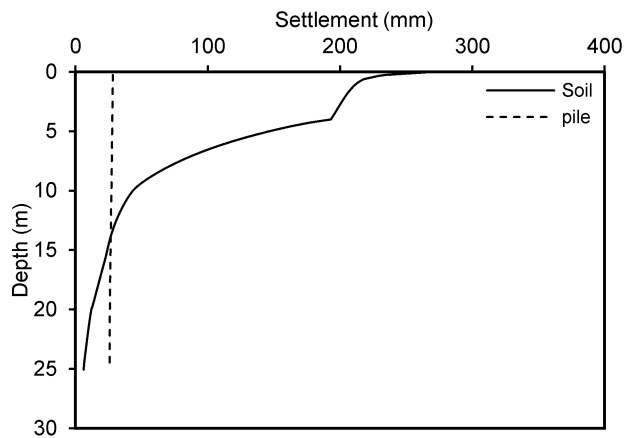
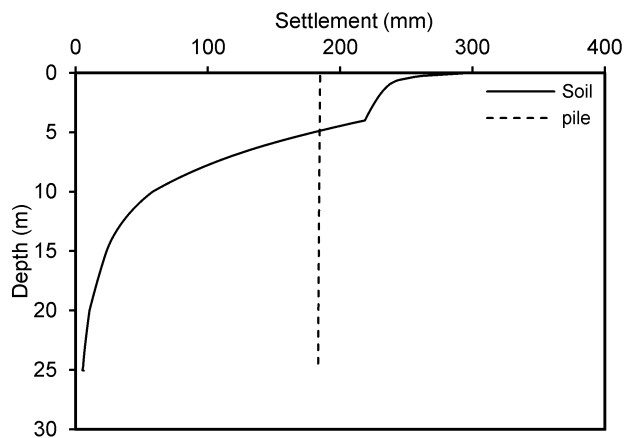


Figure 15. Comparison of axial load distribution on coated and uncoated piles



a) Uncoated pile



b) Coated pile

Figure 15. Comparison of pile and soil settlement for coated and uncoated piles

5 CONCLUSIONS

Finite element analyses were carried out in this paper to investigate negative skin friction on uncoated and coated concrete piles. The study included the effects of pile coating, pile length, and external vertical loading on the location of the neutral plane. Based on the numerical analyses results, the following conclusions can be made:

- Finite element analysis using Plaxis 2D can adequately capture the behaviour of piles subject to negative skin friction.
- A value of $\beta = 0.2$ provides a reasonable estimation of negative skin friction mobilized in soft clay. More accurate estimation of negative skin friction mobilized in soft clay can be predicted using β that varies with depth.
- For piles installed in a compressible soil, the depth of the neutral plane increases with increasing pile length.
- With increasing vertical load on a pile's head, the amount of negative skin friction and the depth of the neutral plane decrease.

ACKNOWLEDGEMENTS

The authors would like to acknowledge the financial support provided by the Ontario Ministry of Transportation in aid of this research.

REFERENCES

- Balasubramaniam, A., Oh, E. Y.N., and Phienwej. 2009. Bored and Driven Pile Testing in Bangkok Sub-Soils. *Lowland Technology International*, 11(1): 29-36.
- Burland, J. 1973. Shaft Friction of Piles in Clay-A Simple Fundamental Approach. *Ground Engineering*, 6(3): 30-42.
- Clemente, F. M. 1981. Downdrag on Bitument Coated Piles in Warm Climate. *10th International Conference on Soil Mechanics and Foundation Engineering*, Stockholm, Sweden, 2:673-676.
- Fellenius, B. H. 1997. Piles Subjected to Negative Friction: A Procedure for Design. Discuaion. *Canadian Geotechnical Engineering*, 28(2): 277-281
- Fellenius, B. H. 2006. Results from Long-Term Measurement in Piles of Drag load and Downdrag. *Canadian Geotechnical Journal*, 43: 409-431.
- Fellenius, B. H. 2015. *Basics of Foundation Design*. Electronic Edition.
- Indraratna, B., Balasubramaniam, A. S., Phamvan, P., & Wong, Y. K. 1992. Development of Negative Skin Friction on Driven Piles in Soft Bangkok Clay. *Canadian Geotechnical Journal*, 29: 393-404.
- Indraratna, B., & Chu, J. 2005. *Ground Improvement-Case Histories*.
- Plaxis 2D. (2012). *Reference Manual*.
- Poulos, H. G. 1979. Group Factors for Pile-Deflection Estimation. *Journal of the Geotechnical Engineering Division*, ASCE, 105 (GT12): 1489-1509.